Nano-Micro Conference

Article View Online

Modeling and Analysis of Bow-Tie Antenna Integrated Resonant-Tunneling-Diode Relaxation Oscillators for Wireless Radio Applications

Hirokazu Yamakura,* Michihiko Suhara*

Department of Electrical and Electronic Engineering, Tokyo Metropolitan University, 1-1, Minami-Osawa, Hachioji, Tokyo, 192-0397 Japan

Corresponding Author. Email: yamakura-hirokazu@ed.tmu.ac.jp, suhara@tmu.ac.jp

Received: 19 May 2017, Accepted: 12 June 2017, Published Online: 15 September 2017

Citation Information: Hirokazu Yamakura, Michihiko Suhara, Nano-Micro Conference, 2017, 1, 01001. doi: 10.11605/cp.nmc2017.01001

Abstract

We propose a self-complementary bow-tie antenna-integrated resonant-tunneling-diode relaxation oscillator and investigate its oscillation/radiation characteristics. In the investigation, we establish a physics-based equivalent circuit model of the oscillator for taking the all physical phenomena related to the diode and the antenna into consideration simultaneously. In this paper, we report the equivalent circuit modeling and the large-signal oscillation/radiation analysis of the oscillator.

Introduction

Terahertz (THz) technology has been received great deal of interest in terms of applications for spectroscopy, imaging, wireless communications, etc. In the wireless communication, the THz range is specifically one of the most attractive regions owing to the existence of the non-allocated frequency band. One of the main challenges of the THz wireless communication is the shortage of the emission RF power of the oscillator. We guess the challenge can be overcome by using the wideband-spectrum relaxation wave, whose entire emission RF power exceeds that of the narrowband sinusoidal wave, as the carrier.

From this perspective, we have proposed an oscillator consisting of a resonant tunneling diode (RTD) and a broadband bow-tie antenna (BTA) [1] for generating a wideband-spectrum relaxation wave and their theoretical models expressed by equivalent circuits respectively [2,3]. Such a semiconductor-based oscillator for THz applications is generally fabricated as a monolithically-integrated configuration of an oscillation device, a radiation antenna, etc. As the performance of such an oscillator depends upon a both of their physics, which usually differ from each other, the performance evaluation method and the design guideline for the oscillator should be established as a physical-coupled scheme considering the all effects regarding the oscillator simultaneously.

In this paper, we focus on a physics-based modeling for the entire oscillator-structure we proposed and its oscillation/radiation performance evaluated by using the physics-based model.

Modeling

Schematics of the proposed oscillator are illustrated in Figure 1.

A peripheral circuit in front serves as a bias circuit and that in back is added for adjusting the total impedance of the peripheral circuits. We establish a physics-based equivalent circuit model of each component, RTD, BTA, and the circuits, since it is considerably impossible to analyze the quantum phenomena of the RTD together with the electromagnetic (EM) properties of the other components by a single solver.

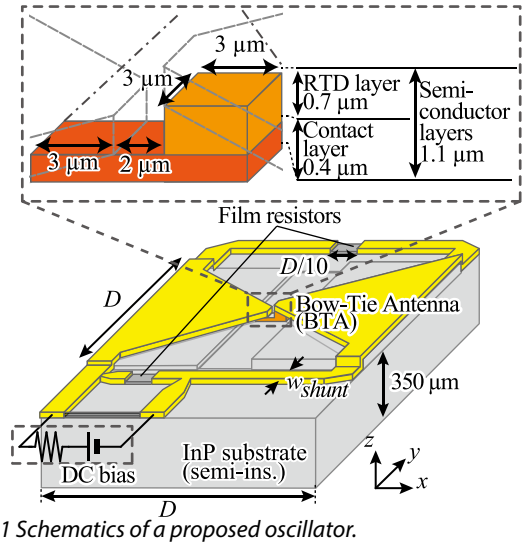

Figure 1 Schematics of a proposed oscillator.

Simple block expressions of the oscillator are described in Figure 2.

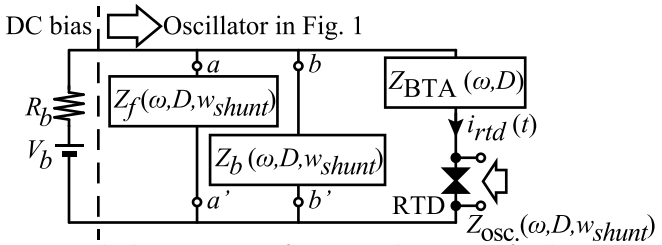

Figure 2 Block expressions of an equivalent circuit for the oscillator shown in Figure 1.

The impedance variables, $Z_f(\omega,D,w_{shunt})$, $Z_b(\omega,D,w_{shunt})$, and $Z_{BTA}(\omega,D)$, correspond to the equivalent circuit of the peripheral circuit in front, that in back, and the BTA, respectively. The RLC expression of $Z_{BTA}(\omega,D)$ has been reported in Ref. [2]. Additionally, the circuit model of the RTD and its theoretical expression has also been reported in Refs. [3, 4], respectively.

The variables, $Z_f(\omega,D,w_{shunt})$ and $Z_b(\omega,D,w_{shunt})$, are com-

doi: 10.11605/cp.nmc2017.01001

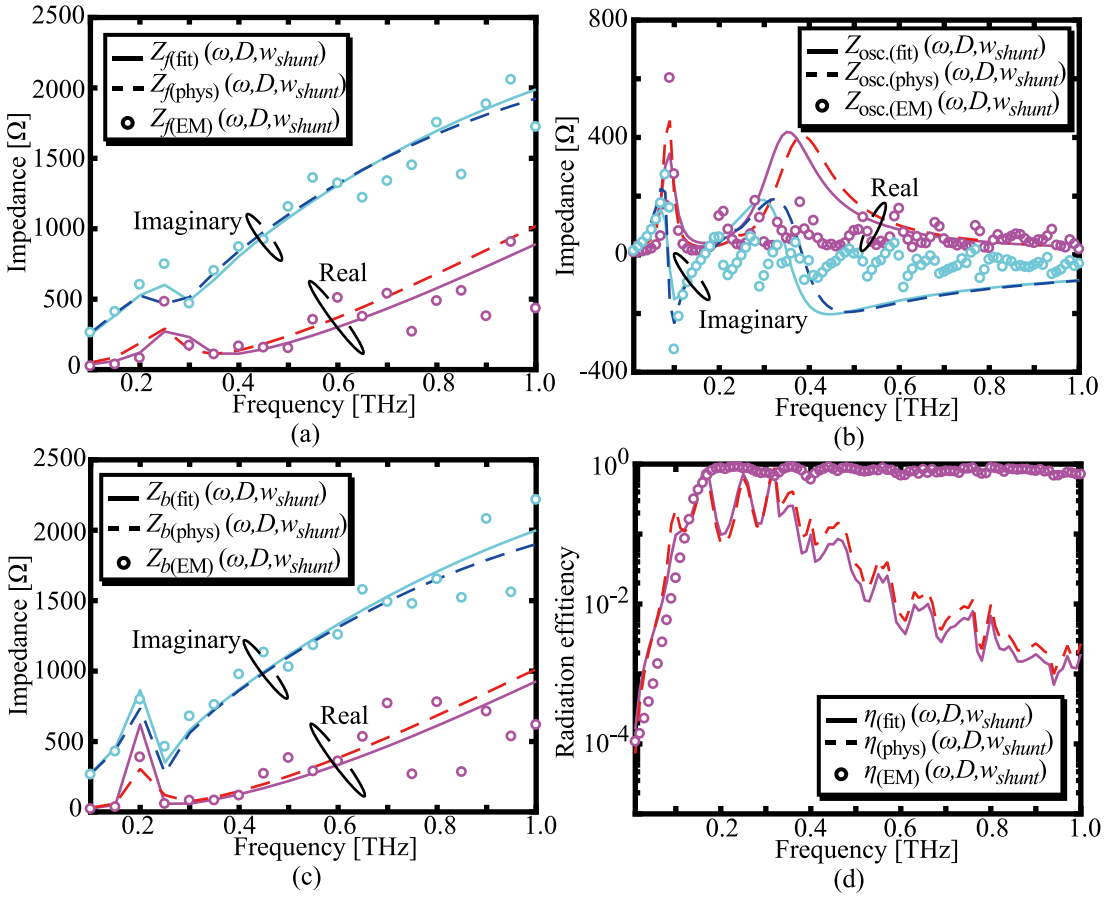

Figure 3 Typical fitting results regarding the impedance characteristics of (a) the peripheral circuit in front, (b) that in back, and (c) the entire oscillator, and (d) the radiation characteristics. Radiation efficiency, $\eta(\omega,D,w_{shunt})$, is defined by the ratio of the oscillation power on the semiconductor layers to the radiation power on the BTA. Solid lines are depicted by using the de-embedded values of the circuit parameters. Dash lines are calculated by the physical/material parameters. The antenna size, D, and the line width, w_{shunt}, are set to 300 and 10 μm, respectively.

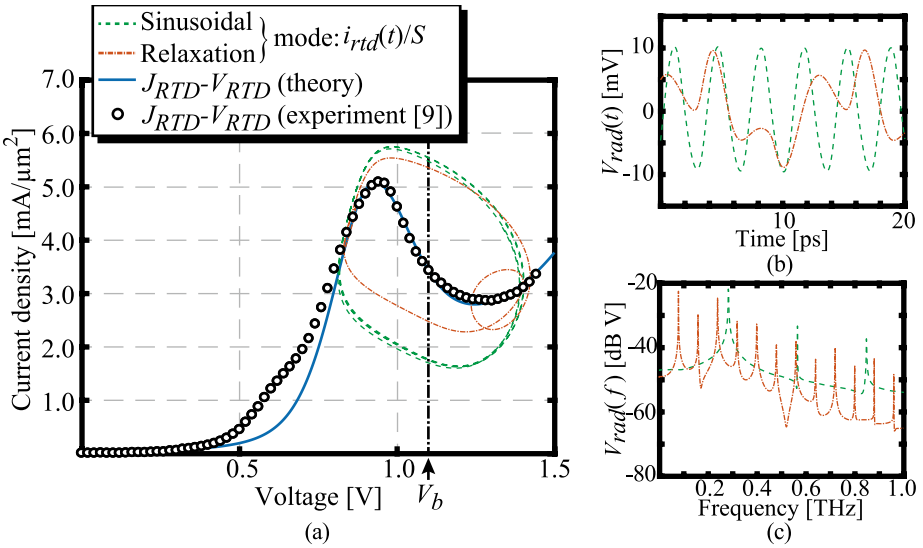

Figure 4 (a) Measured/theoretical current density-voltage (J-V) characteristics of the employed RTD and the calculated results of the time-dependent orbit of the current density, $i_{rtd}(t)/S$, in the RTD. (b) Waveforms of the radiation voltage and (c) corresponding frequency spectra. Chain and dotted lines indicate the relaxation and the sinusoidal oscillation mode, where the line width, w_{shunt}, is set to 10 and 20 μm, respectively. Antenna size, D, is set to 300 μm.

posed of several RLC elements which can be explained by the electromagnetic properties: the surface impedance due to the skin effect [5], the straight micro stripline [6], fringe capacitance [7], and parasitic components regarding the semi-insulating substrate. The circuit elements involved in $Z_f(\omega,D,w_{shunt})$ and $Z_b(\omega,D,w_{shunt})$ are evaluated by the EM field distribution in the vicinity of the circuits calculated by the finite element method-based simulator, namely, COMSOL. Their approximate numerical values of the elements are also estimated by the physical interpretation based on the structural and material properties. More precise values are numerically de-embedded by using the optimization method, namely, the particle swarm optimization [8]. More details regarding the circuit identification process have also been reported in Ref. [2].

Figure 3 summarizes the typical fitting results of the im-

Published by Nature Research Society http://nrs.org

doi: 10.11605/cp.nmc2017.01001

pedance and radiation characteristics regarding the peripheral circuit/entire oscillator.

From Figure 3, the equivalent circuit expression is quantitatively valid for the evaluation of the radiation/oscillation characteristics by the circuit analysis around the first resonance frequency of the oscillator.

Oscillation Analysis

The non-linear oscillation analysis of the proposed oscillator is performed by using the equivalent circuit above mentioned. The non-linearity of the RTD is involved by

considering the measured current-voltage (I-V) charact-eristics [9]. The supplied voltage, V_b, is set to a constant value to keep the negative differential conductance of the RTD maximum. More details regarding the oscillation analysis methodology have been reported in Refs. [10, 11].

Figure 4 displays the current density-voltage (J-V) charact-eristics of the RTD and the time-dependent orbit of the current density, $i_{rtd}(t)/S$, in the RTD, where S indicates the mesa area.

We classify the oscillation modes depicted the dotted and chain lines in Figure 4 designated as the "sinusoidal" and the "relaxation" mode, respectively. The modes are quantitatively distinguished by the cycle number of the $i_{rtd}(t)/S$ trajectory in Figure 4; if the cycle number is unity, the mode is a “sinusoidal mode”; else, it is a “relaxation mode”. The entire emission RF power of the relaxation mode shown in Figure 4 is ~ 6 dBm greater than that of the sinusoidal mode when the upper limit value of band is approximately set to 400 GHz. It is suggested that the relaxation wave can compensate for the shortage of the emission RF power if we employ a certain band appropriately. Moreover, it is found that the oscillation mode can be designed by adjusting the two parameters, D and w_{shunt}, appropriately.

According to Shannon-Hartley theorem [12], the capacity of a wireless channel is directly proportional to the channel bandwidth. Therefore, the wideband-spectrum relaxation wave can contribute to the possibility of large-capacity wireless transmissions together with compensating for the RF power shortage.

Conclusion

We investigated radiation/oscillation characteristics of the resonant tunneling diode-based relaxation oscillator by using its physics-based equivalent circuit model. The advantage of a wideband-spectrum relaxation wave as the carrier was revealed in terms of the entire emission RF power. Our further studies will represent the link-budget analysis of the relaxation carrier wave-based THz wireless link to clarify the advantage of the relaxation carrier regarding the link performance.

References

[1] H. Yamakura, Y, Ishiguro, Y. Kato, M. Suhara. 41-th International Conference of Infrared, Millimeter, and THz waves. M5P.12.24, Sept., 2016. doi: 10.1109/IRMMW-THz.2016.7758647

[2] H. Yamakura, M. Suhara. IEICE Transactions on Electronics. 2016, E99-C(12), 1312-1322. doi: 10.1587/transele.E99.C.1312

[3] K. Asakawa, M. Naoi, Y. Iki, M. Shinada, M. Suhara. Physica Status Solidi (C). 2010, 7(10), 2555-2558. doi:10.1002/pssc.200983885

[4] H. Shin-ya, M. Suhara, N. Asaoka, M. Naoi. IEICE Transactions on Electronics. 2010, E93-C(8), 1295-1301. doi:10.1587/transele.E93.C.1295

[5] J. J. Sanz-Fernandez, R. Cheung, G. Goussetis, C. Mateo-Segura. IEEE Transactions on Antennas and Propagation. 2011, 59(6), 2205-2216. doi:10.1109/TAP.2011.2143654

[6] I. Bahl, P. Bhartia. Microwave solid state circuit design, 2nd edition, pp.59, Wiley, 2003.

[7] S.H. Kim, J.G. Fossum, J.W. Yang. IEEE Transactions on Electron Devices. 2006, 53(9), 2143-2150. doi: 10.1109/TED.20006.880369

[8] J. Kennedy and R. Eberhart. Proceedings of IEEE International Conference on Neural Networks. 1995, 4, 1942-1948. doi: 10.1109/ICNN.1995.488968

[9] M. Reddy, S. C. Martin, A. C. Molnar, R. E. Muller, R. P. Smith, P. H. Siegel, M. J. Mondry, M. J. W. Rodwell, H. Kroemer, S. J. Allen. IEEE Electron Device Letters. 1997, 18(5), 218-221. doi: 10.1109/55.568771

[10] K. Asakawa, Y. Itagaki, H. Shin-ya, M. Saito, M. Suhara. IEICE Transactions on Electronics. 2012, E95-C(8), 1376-1384. doi:10.1587/transele.E95.C.1376

[11] N. Okumura, K. Asakawa, M. Suhara. IEICE Transactions on Electronics. 2017, E100-C(5), 430-438. doi: 10.1587/transele.E100.C.430

[12] C. E. Shannon. Tee Bell System Technical Journal. 1948, 27(3), 379-423. doi: 10.1002/j.1538-7305.1948.tb01338.x